



Supplement of

An intercomparison of satellite, airborne, and ground-level observations with WRF–CAMx simulations of NO₂ columns over Houston, Texas, during the September 2021 TRACER-AQ campaign

M. Omar Nawaz et al.

Correspondence to: M. Omar Nawaz (nawaz.muhammad@email.gwu.edu)

The copyright of individual parts of the supplement might differ from the article licence.

Section S1. Supplementary Tables and Figures

Table S1: WRF physics options and data sources

WRF Option	Option Selected
Analysis Data	0.25° GDAS (IC/BCs and analysis nudging on the 36 and 12 km domains)
Microphysics	Thompson
Longwave Radiation	Rapid Radiative Transfer Model (RRTMG)
Shortwave Radiation	RRTMG
Surface Layer Physics	Revised MM5 surface layer scheme
LSM	Noah
PBL scheme	Yonsei University (YSU)
Cumulus scheme	Multi-Scale Kain-Fritsch (MSKF) on 36/12 km; none for 4/1.333/0.444 km

Table S2: Vertical layer mapping from WRF to CAMx

WRF Layer No.	WRF Eta Level	WRF Layer Pressure (mb)	WRF Layer Top (m)	CAMx Layer No.	CAMx Layer Top (m)	CAMx Layer Thickness (m)
44	0.000	50.00	20576			
43	0.010	59.63	19458			
42	0.025	74.08	18082	30	18082	3885
41	0.045	93.35	16616			
40	0.065	112.61	15427			
39	0.090	136.69	14198	29	14198	2977
38	0.115	160.77	13169			
37	0.145	189.67	12120			
36	0.175	218.57	11221	28	11221	1850
35	0.210	252.28	10304			
34	0.250	290.81	9372	27	9372	1599
33	0.290	329.34	8534			
32	0.330	367.87	7773	26	7773	1269
31	0.370	406.40	7073			
30	0.405	440.12	6504	25	6504	1040
29	0.440	473.83	5969			
28	0.475	507.54	5464	24	5464	870
27	0.510	541.26	4985			
26	0.540	570.16	4594	23	4594	737
25	0.570	599.05	4219			
24	0.600	627.95	3857	22	3857	684
23	0.630	656.85	3509			
22	0.660	685.75	3174	21	3174	325
21	0.690	714.64	2849	20	2849	314
20	0.720	743.54	2535	19	2535	304
19	0.750	772.44	2231	18	2231	247
18	0.775	796.52	1984	17	1984	241
17	0.800	820.60	1744	16	1744	235
16	0.825	844.68	1509	15	1509	230
15	0.850	868.76	1279	14	1279	135
14	0.865	883.21	1144	13	1144	134
13	0.880	897.66	1010	12	1010	132
12	0.895	912.11	878	11	878	130
11	0.910	926.56	748	10	748	86
10	0.920	936.19	662	9	662	85
9	0.930	945.82	577	8	577	84

8	0.940	955.46	493	7	493	84
7	0.950	965.09	409	6	409	83
6	0.960	974.72	326	5	326	82
5	0.970	984.35	243	4	243	82
4	0.980	993.99	162	3	162	81
3	0.990	1003.62	81	2	81	48
2	0.996	1009.40	32	1	32	32
1	0.998	1011.32	16			
surface	1.000	1013.25	0	0	0	

20 **Table S3: Science options for the CAMx simulation**

Science Options	CAMx Configuration
Version	Version 7.20
Time Zone	CST
Vertical Grid Mesh	30 Layers with 32 m deep surface layer and 15 layers in the lowest 1.5 km
Horizontal Grids	2-way nested grids with spacings of 1.333 and 0.444 km
Meteorology	2021 WRF meteorology
Chemistry Mechanism	CB6r5 gas-phase mechanism
Chemistry Solver	EBI
Probing Tool	Ozone Source Apportionment Technology (OSAT)
Photolysis Rates	TUV version 4.8 with TOMS ozone column adjustment and in-line adjustment for clouds
Advection Scheme	Piecewise Parabolic Method (PPM)
Planetary Boundary Layer (PBL) mixing	K-theory with KV100 patch to enhance vertical mixing over urban areas within the lowest 100 m
In-line Ix Emissions On	Inorganic iodine (Ix) emissions from saltwater areas
Parallelization	MPI (18 threads) and OMP (6 threads)

Table S4: Major energy generation units in and around Houston, TX and their monthly NO_x emissions

Number	Energy Generation Unit	NO _x (tons/month)
1	Air Liquide Bayport Complex	570.7
2	Cedar Bayou	73.0
3	W A Parish	34.7
4	Odyssey Energy Altura Cogen, LLC	34.6
5	Texas City Cogeneration	30.8
6	Pasadena Power Plant	27.4
7	Channelview Cogeneration Facility	25.9
8	Deer Park Energy Center	25.0
9	South Houston Green Power Site	25.0
10	TH Wharton	18.1
11	Greens Bayou	11.6

25

Table S5: Comparison of observed (OBS) and simulated (WRF) wind direction and associated statistics. Red shading indicates days with limited GCAS observations due to cloud coverage. The statistical measures of mean bias error (MBE), mean absolute error (MAE), and Pearson-R squared (R^2) are computed using the astropy circular statistics python module (<https://docs.astropy.org/en/stable/stats/circ.html>).

Date	WRF Dir (°)	OBS Dir (°)	R^2	MBE	MAE	N
09/01	184.0	180.0	0.04	-1.0	36.0	130
09/03	136.0	185.0	-0.04	-49.0	60.0	137
09/08	13.0	17.0	0.57	-10.0	29.0	137
09/09	20.0	37.0	0.78	-11.0	24.0	149
09/10	81.0	75.0	0.38	6.0	17.0	149
09/11	89.0	92.0	0.68	-3.0	14.0	151
09/23	63.0	88.0	0.3	-24.0	28.0	118
09/24	87.0	97.0	0.47	-8.0	20.0	137
09/25	70.0	59.0	0.57	9.0	24.0	114
09/26	97.0	96.0	0.8	0.0	19.0	117
All Days	82.0	87.0	0.76	-8.0	26.0	1339
Not Cloudy Days	67.0	73.0	0.73	-5.0	21.0	1072

30

Table S6: Comparison of observed (OBS) and simulated (WRF) wind speed and associated statistics. Red shading indicates days with limited GCAS observations due to cloud coverage. The statistical measures of mean bias error (MBE), mean absolute error (MAE), and Pearson-R squared (R^2) are defined at the end of this supplement in section S2.

35

Date	WRF Spd (m/s)	OBS Spd (m/s)	R^2	MBE	MAE	N
09/01	3.47	2.93	0.07	0.55	1.51	145
09/03	3.46	3.17	0.0	0.29	1.8	151
09/08	3.46	2.79	0.1	0.68	1.25	150
09/09	3.7	3.76	0.23	-0.06	0.94	152
09/10	4.6	4.69	0.5	-0.09	0.98	149
09/11	4.11	5.04	0.32	-0.93	1.35	151
09/23	3.14	3.2	0.2	-0.06	1.17	130
09/24	3.32	3.77	0.41	-0.45	0.96	142
09/25	2.73	2.66	0.25	0.07	0.94	135
09/26	3.1	3.29	0.36	-0.2	0.99	131
All Days	3.53	3.55	0.26	-0.02	1.2	1436
Not Cloudy Days	3.55	3.68	0.37	-0.13	1.08	1140

40

Table S7: Comparison of observed (OBS) and simulated (WRF) temperature and associated statistics. Red shading indicates days with limited GCAS observations due to cloud coverage. The statistical measures of mean bias error (MBE), mean absolute error (MAE), and Pearson-R squared (R^2) are defined at the end of this supplement in section S2.

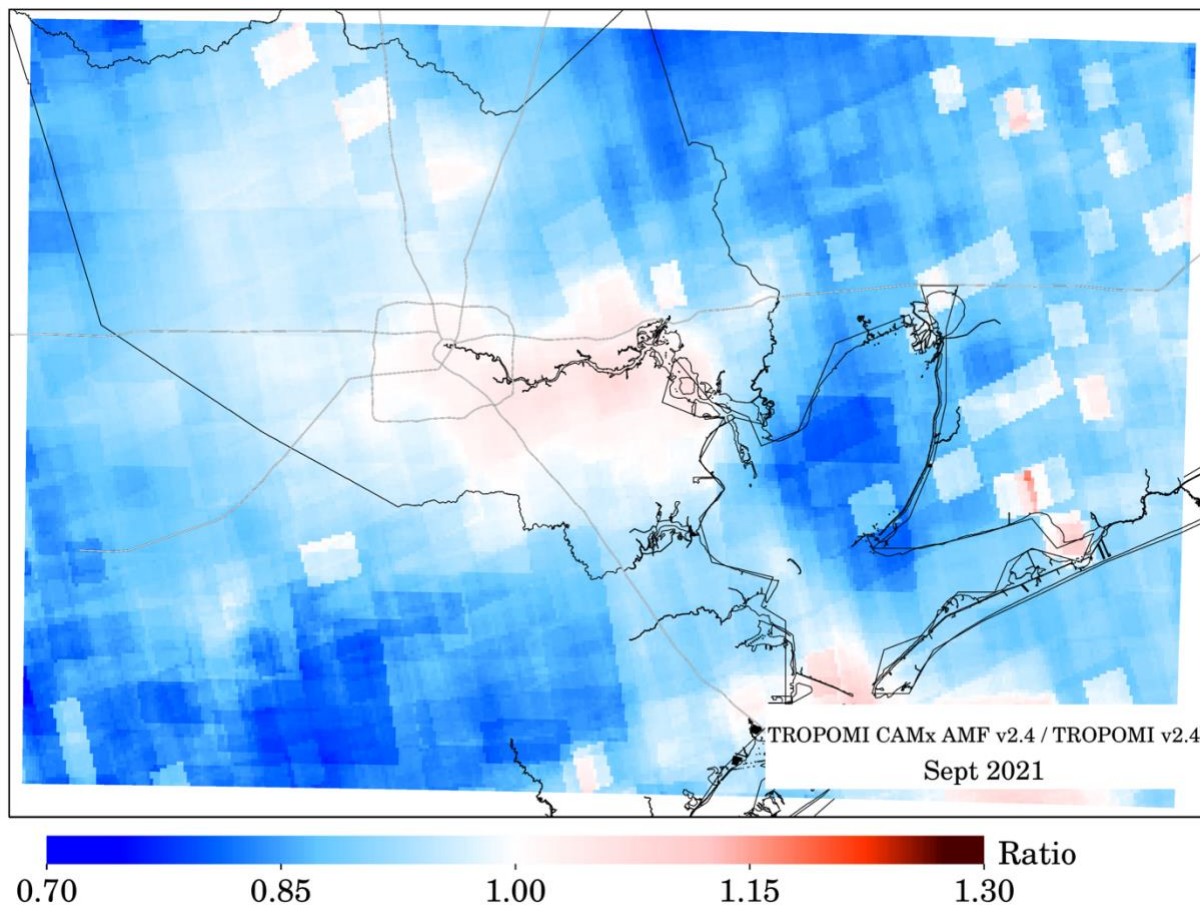
Date	WRF Temp (K)	OBS Temp (K)	R^2	MBE	MAE	N
09/01	305.5	304.2	0.0	1.3	2.28	159
09/03	305.0	303.0	0.0	1.99	2.61	158
09/08	304.5	304.1	0.75	0.42	1.16	160
09/09	305.1	304.4	0.78	0.66	1.15	160
09/10	303.1	303.2	0.76	-0.1	0.93	158
09/11	302.5	302.3	0.74	0.18	0.99	157
09/23	298.4	298.6	0.69	-0.26	1.14	147
09/24	299.2	299.3	0.72	-0.11	1.02	150
09/25	299.5	299.9	0.81	-0.33	1.02	148
09/26	300.0	300.1	0.69	-0.02	1.18	150
All Days	302.4	302.0	0.71	0.39	1.35	1547
Not Cloudy Days	301.6	301.5	0.86	0.06	1.07	1230

45

Table S8: Comparison of observed (OBS) and simulated (WRF) water vapor mixing ratio (WVMR) and associated statistics. Red shading indicates days with limited GCAS observations due to cloud coverage. The statistical measures of mean bias error (MBE), mean absolute error (MAE), and Pearson-R squared (R^2) are defined at the end of this supplement in section S2.

Date	WRF WVMR (g/kg)	OBS WVMR (g/kg)	R^2	MBE	MAE	N
09/01	17.5	19.4	0.26	-1.92	1.97	99
09/03	17.7	18.6	0.21	-0.88	1.22	98
09/08	12.3	12.2	0.78	0.09	1.31	100
09/09	10.7	13.8	0.28	-3.07	3.11	100
09/10	9.1	10.7	0.67	-1.51	1.6	98
09/11	10.6	12.6	0.21	-2.03	2.28	97
09/23	6.0	7.6	0.54	-1.55	1.58	97
09/24	7.4	8.8	0.32	-1.34	1.46	100
09/25	8.2	9.7	0.54	-1.51	1.53	98
09/26	10.8	11.6	0.48	-0.76	0.87	100
All Days	11.1	12.5	0.85	-1.45	1.69	987
Not Cloudy Days	9.4	10.9	0.64	-1.46	1.72	790

50



55 **Figure S1: Ratio of TROPOMI NO₂ columns during September 2021 with the new CAMx AMF compared to the operational AMF.**

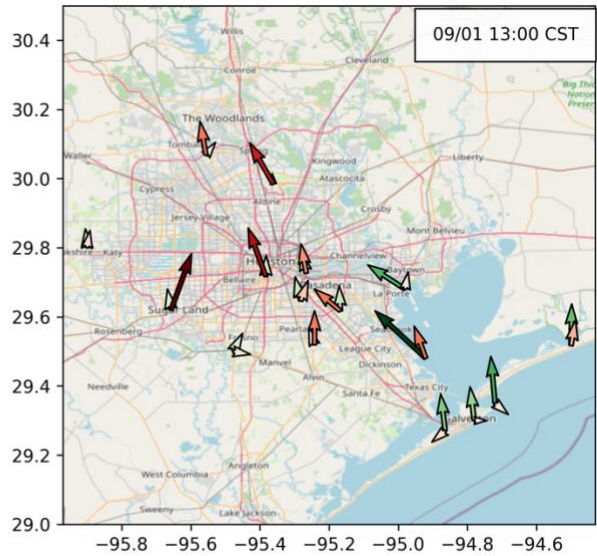
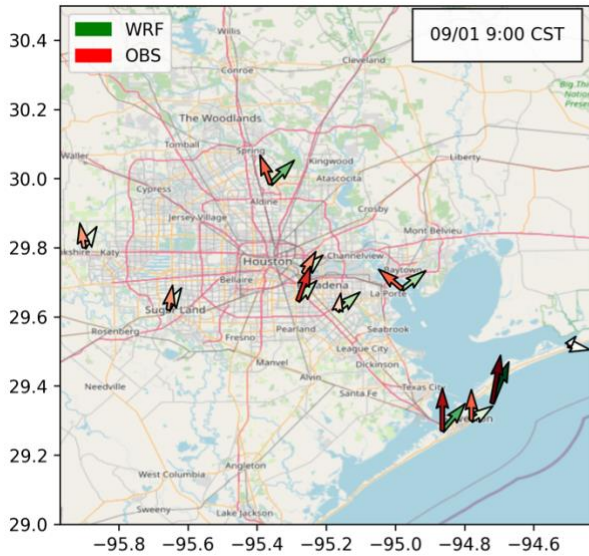


Figure S2: Comparison of observed (OBS) and simulated (WRF) wind at 9am and 1pm CST across sixteen ground-level monitors on September 1, 2021. © OpenStreetMap contributors 2023. Distributed under the Open Data Commons Open Database License (ODbL) v1.0.

60

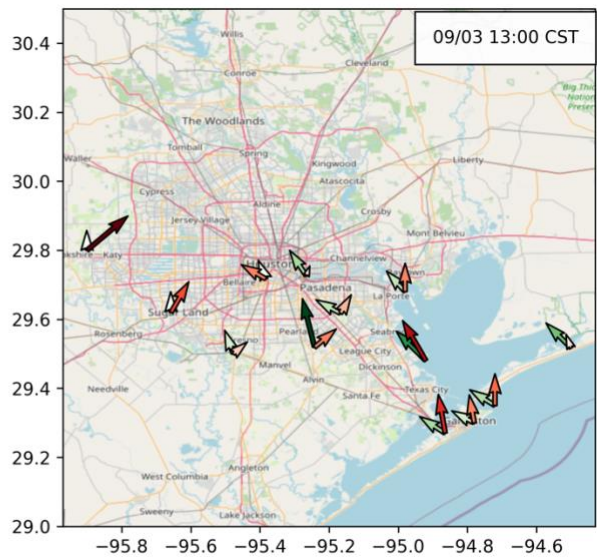
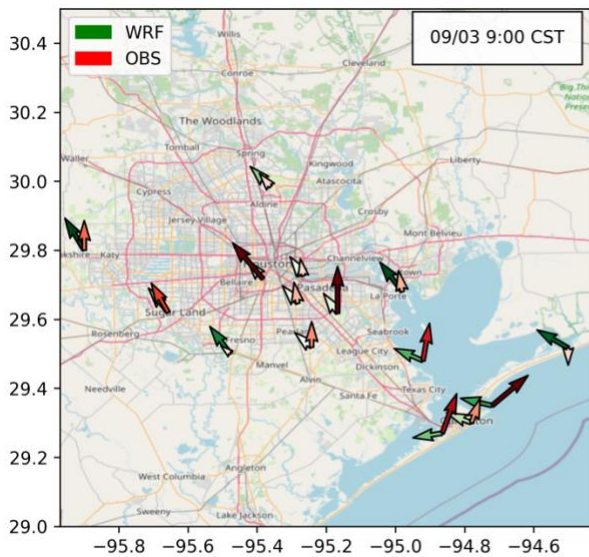
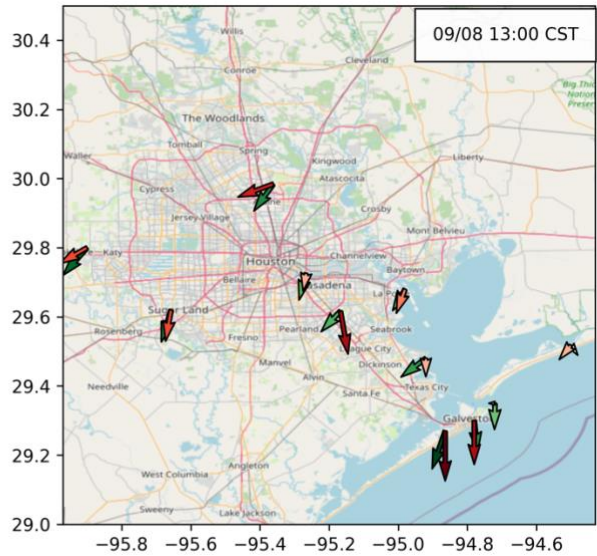
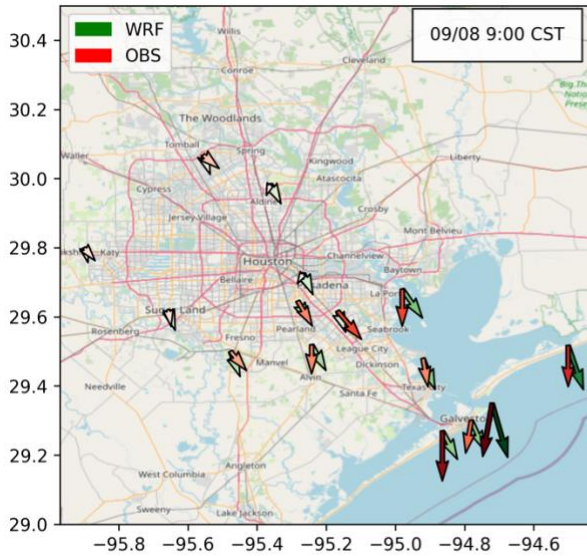
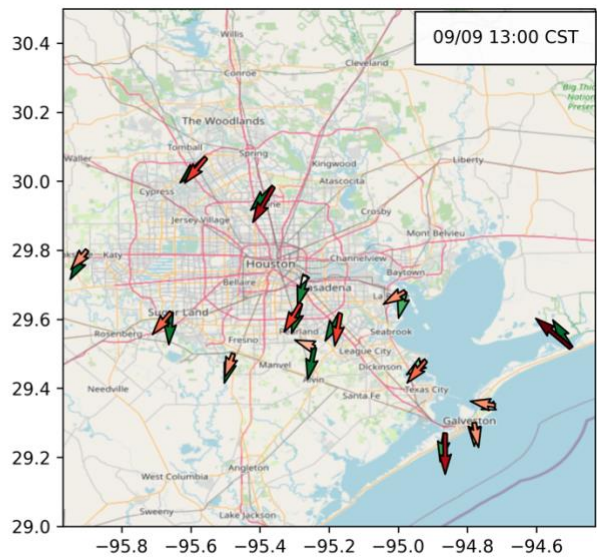
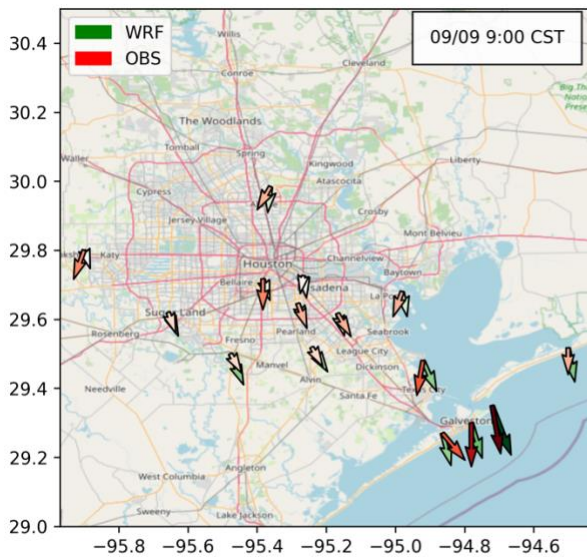


Figure S3: Comparison of observed (OBS) and simulated (WRF) wind at 9am and 1pm CST across sixteen ground-level monitors on September 3, 2021. © OpenStreetMap contributors 2023. Distributed under the Open Data Commons Open Database License (ODbL) v1.0.

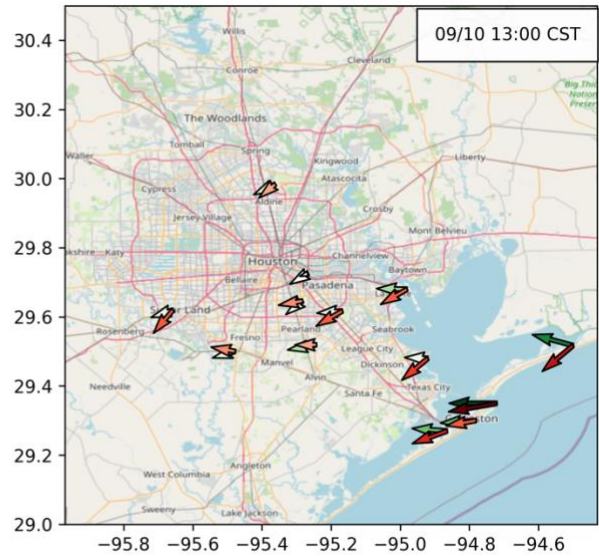
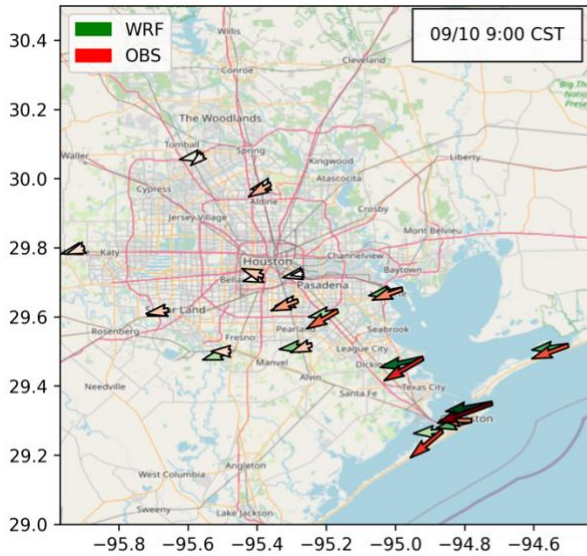
65



70 **Figure S4: Comparison of observed (OBS) and simulated (WRF) wind at 9am and 1pm CST across sixteen ground-level monitors on September 8, 2021. © OpenStreetMap contributors 2023. Distributed under the Open Data Commons Open Database License (ODbL) v1.0.**



75 **Figure S5: Comparison of observed (OBS) and simulated (WRF) wind at 9am and 1pm CST across sixteen ground-level monitors on September 9, 2021. © OpenStreetMap contributors 2023. Distributed under the Open Data Commons Open Database License (ODbL) v1.0.**



80

Figure S6: Comparison of observed (OBS) and simulated (WRF) wind at 9am and 1pm CST across sixteen ground-level monitors on September 10, 2021. © OpenStreetMap contributors 2023. Distributed under the Open Data Commons Open Database License (ODbL) v1.0.

85

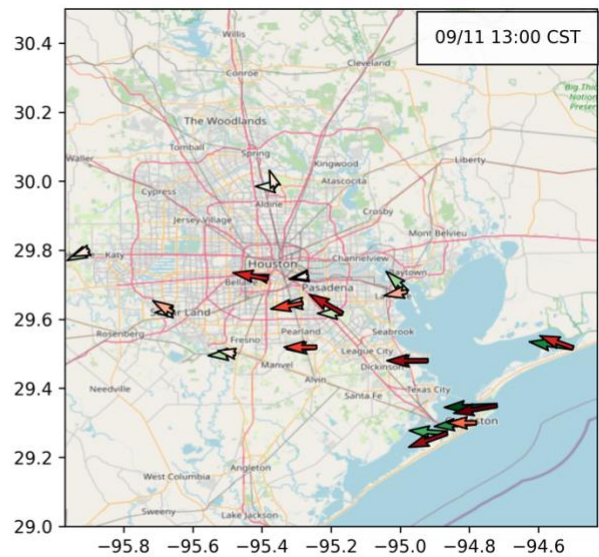
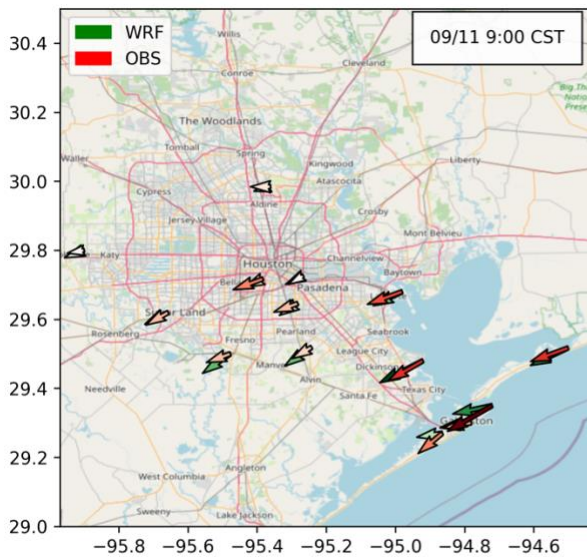


Figure S7: Comparison of observed (OBS) and simulated (WRF) wind at 9am and 1pm CST across sixteen ground-level monitors on September 11, 2021. © OpenStreetMap contributors 2023. Distributed under the Open Data Commons Open Database License (ODbL) v1.0.

90

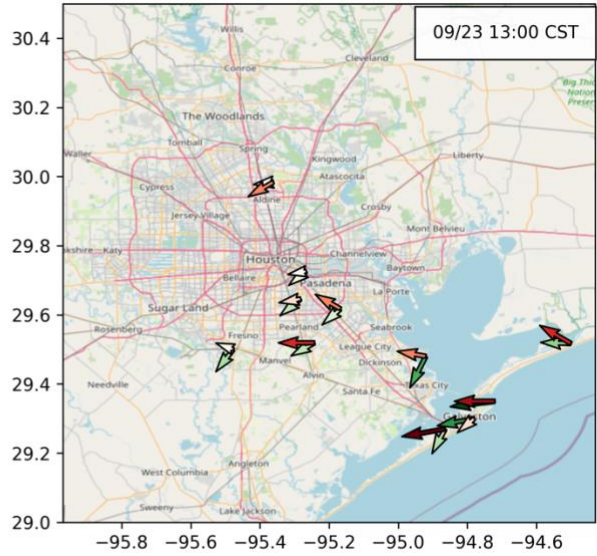
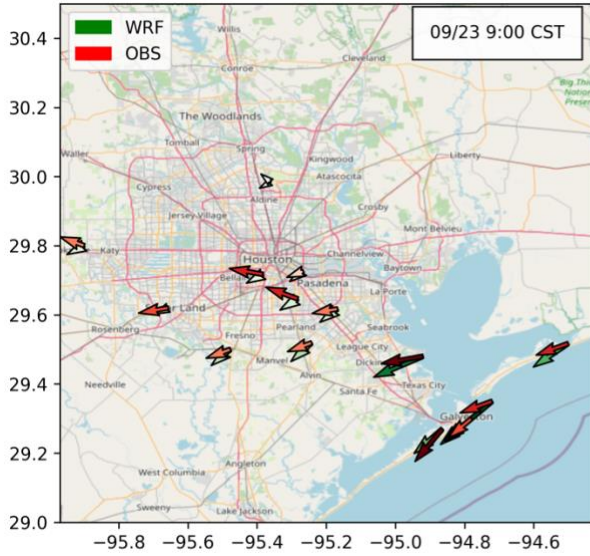


Figure S8: Comparison of observed (OBS) and simulated (WRF) wind at 9am and 1pm CST across sixteen ground-level monitors on September 23, 2021. © OpenStreetMap contributors 2023. Distributed under the Open Data Commons Open Database License (ODbL) v1.0.

95

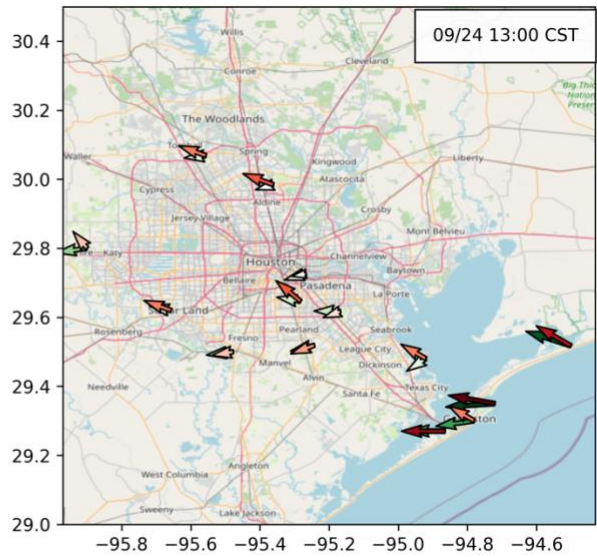
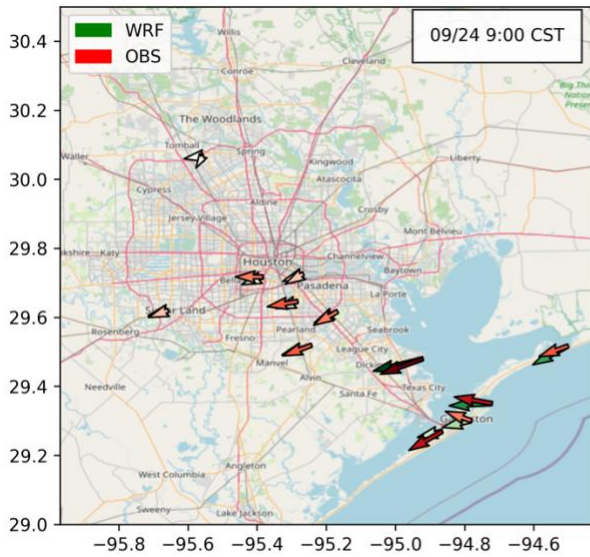
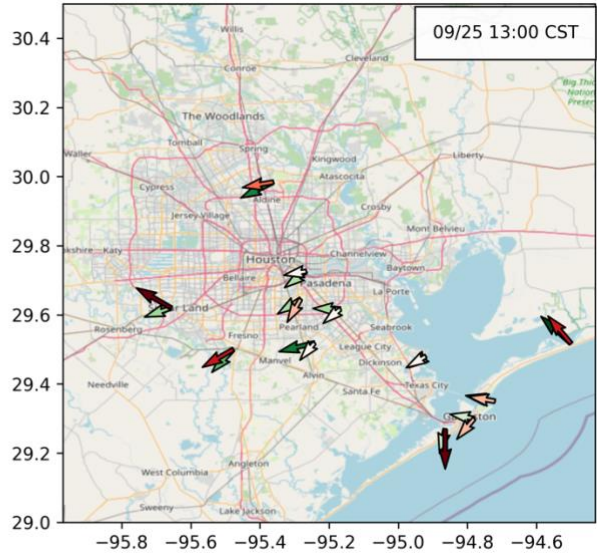
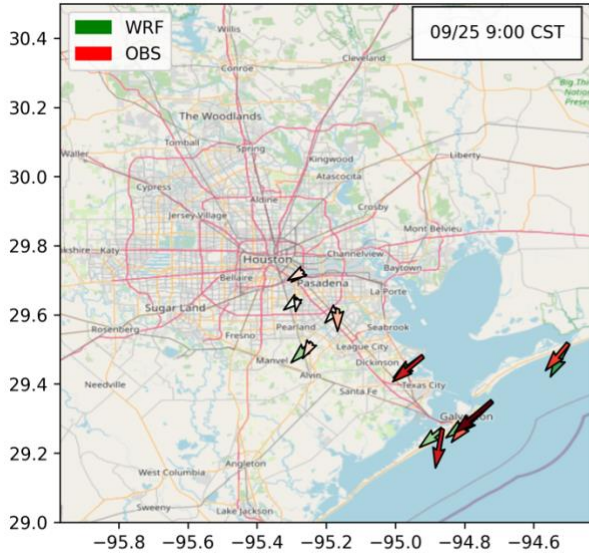
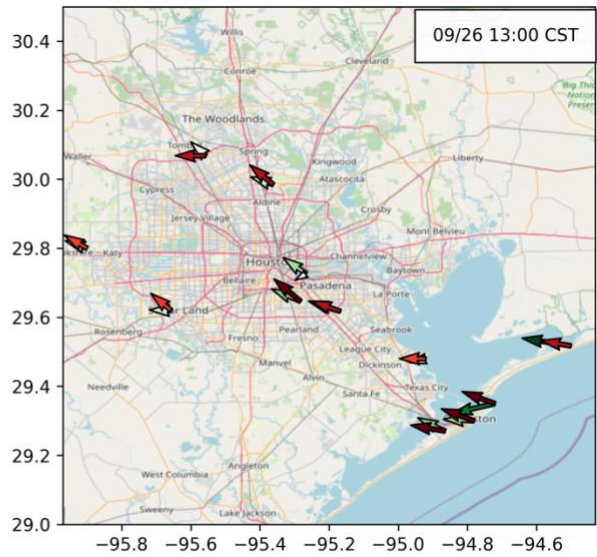
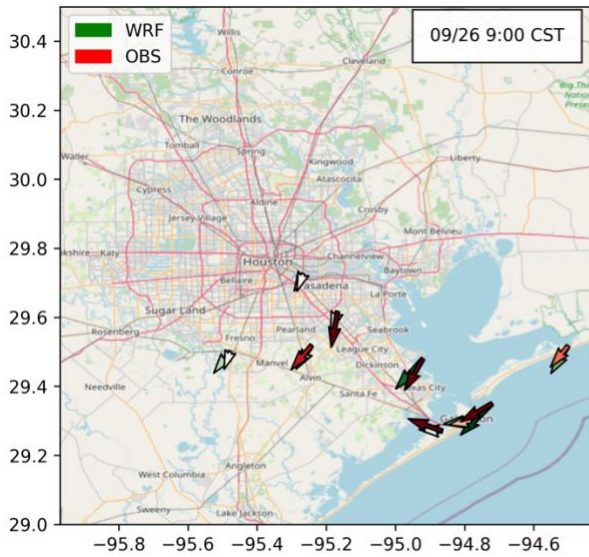


Figure S9: Comparison of observed (OBS) and simulated (WRF) wind at 9am and 1pm CST across sixteen ground-level monitors on September 24, 2021. © OpenStreetMap contributors 2023. Distributed under the Open Data Commons Open Database License (ODbL) v1.0.

100

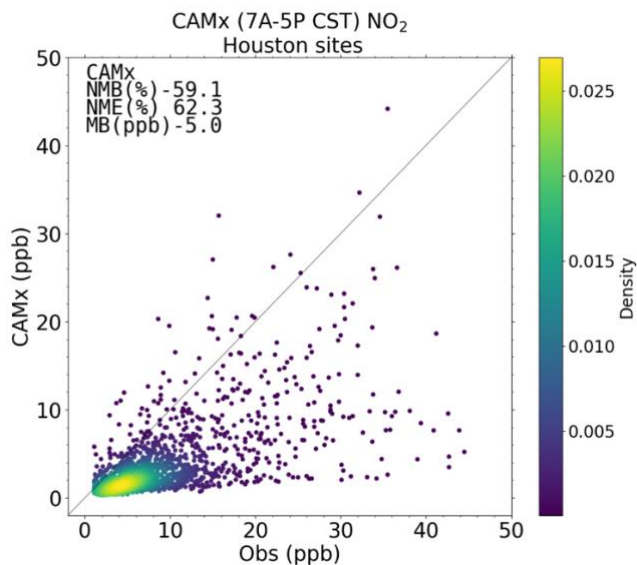


105 **Figure S10: Comparison of observed (OBS) and simulated (WRF) wind at 9am and 1pm CST across sixteen ground-level monitors on September 25, 2021. © OpenStreetMap contributors 2023. Distributed under the Open Data Commons Open Database License (ODbL) v1.0.**

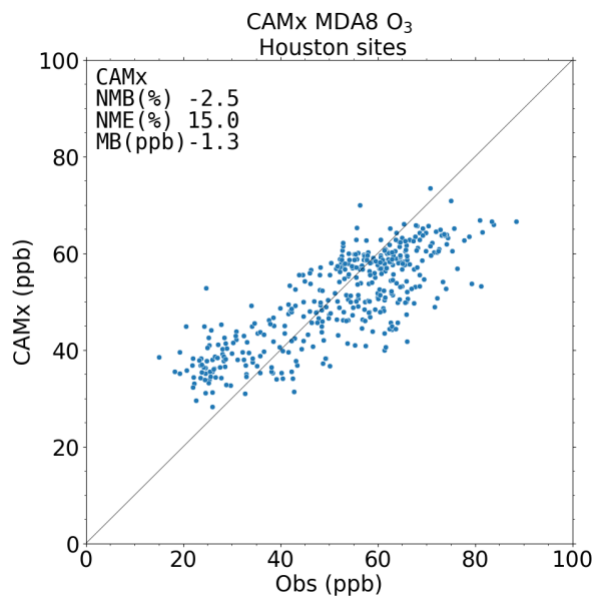


110 **Figure S11: Comparison of observed (OBS) and simulated (WRF) wind at 9am and 1pm CST across sixteen ground-level monitors on September 26, 2021. © OpenStreetMap contributors 2023. Distributed under the Open Data Commons Open Database License (ODbL) v1.0.**

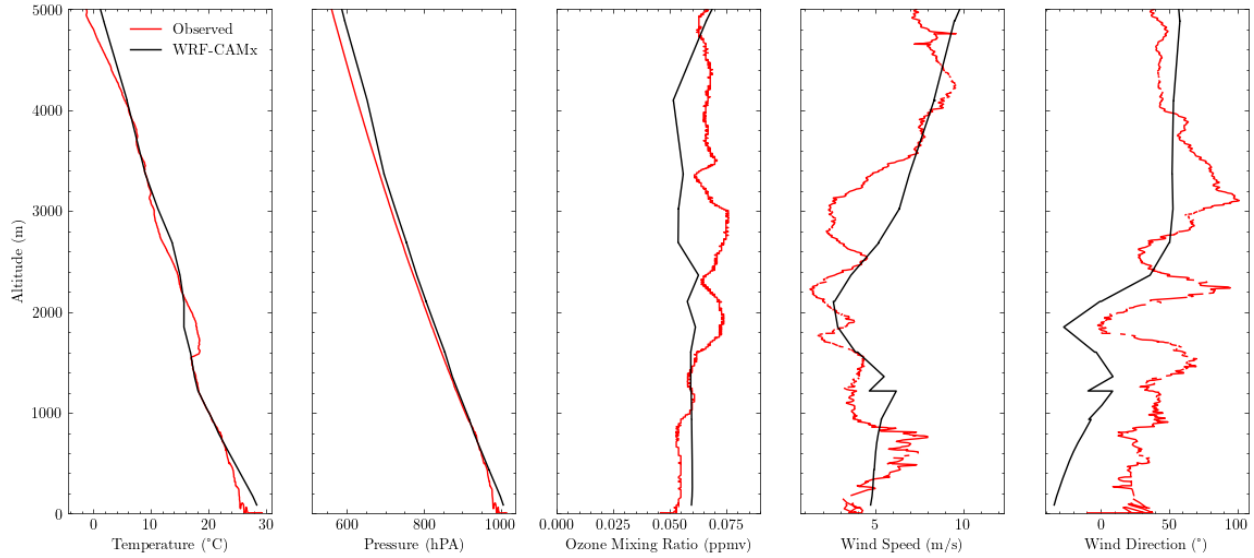
115



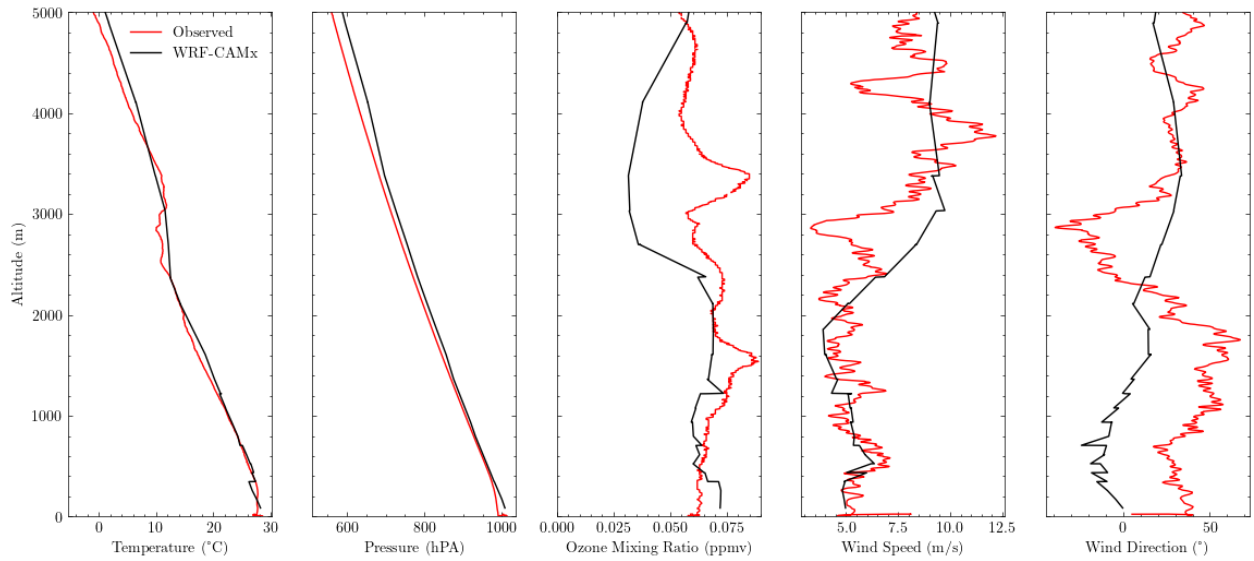
120 **Figure S12: Hourly CAMx (7 AM-5 PM CST) surface NO₂ plotted against observed surface NO₂ across all TCEQ CAMS sites within Houston for all days with GCAS flight measurements during the August 30-September 27, 2021 modeling period.**



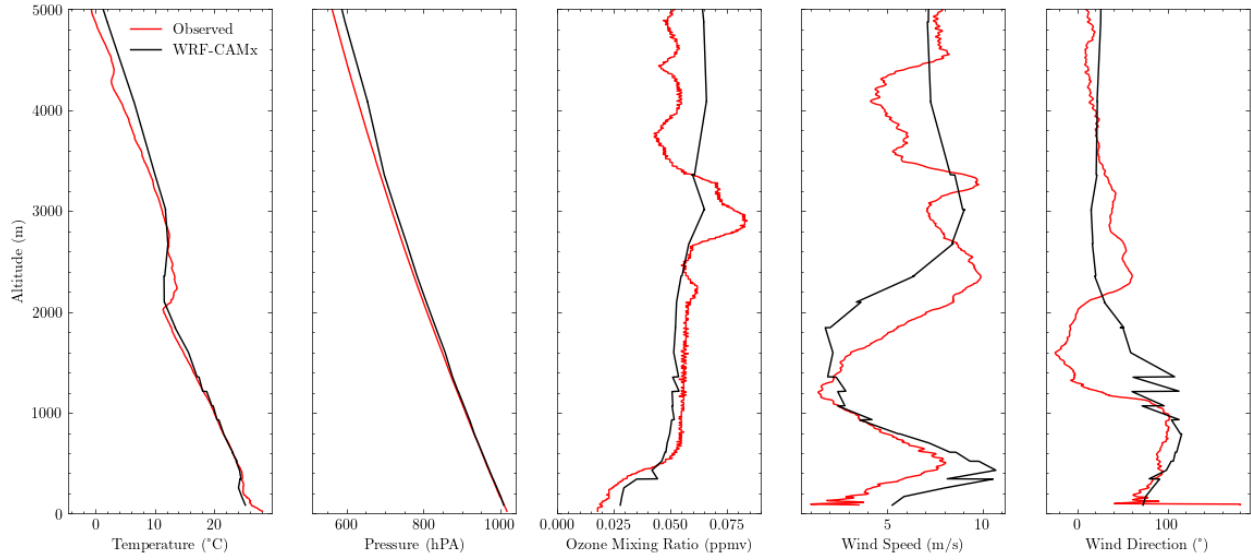
125 **Figure S13. MDA8 CAMx simulated and observed surface-level ozone across all TCEQ CAMS sites within Houston for all days with GCAS flight measurements during the August 30-September 27, 2021 modeling period.**



130 **Figure S14: Comparison between WRF-CAMx simulated meteorology and ozone mixing ratios and ozonesondes observations at 11 am on 9/8 at 29.324° N and 94.552° W (Gulf)**



135 **Figure S15: Comparison between WRF-CAMx simulated meteorology and ozone mixing ratios and ozonesondes observations at 10am on 9/9 at 29.383° N and 94.831° W (Galveston Bay)**



140

Figure S16: Comparison between WRF-CAMx simulated meteorology and ozone mixing ratios and ozonesondes observations at 8am on 9/10 at 29.724° N and 95.339° W (University of Houston)

145

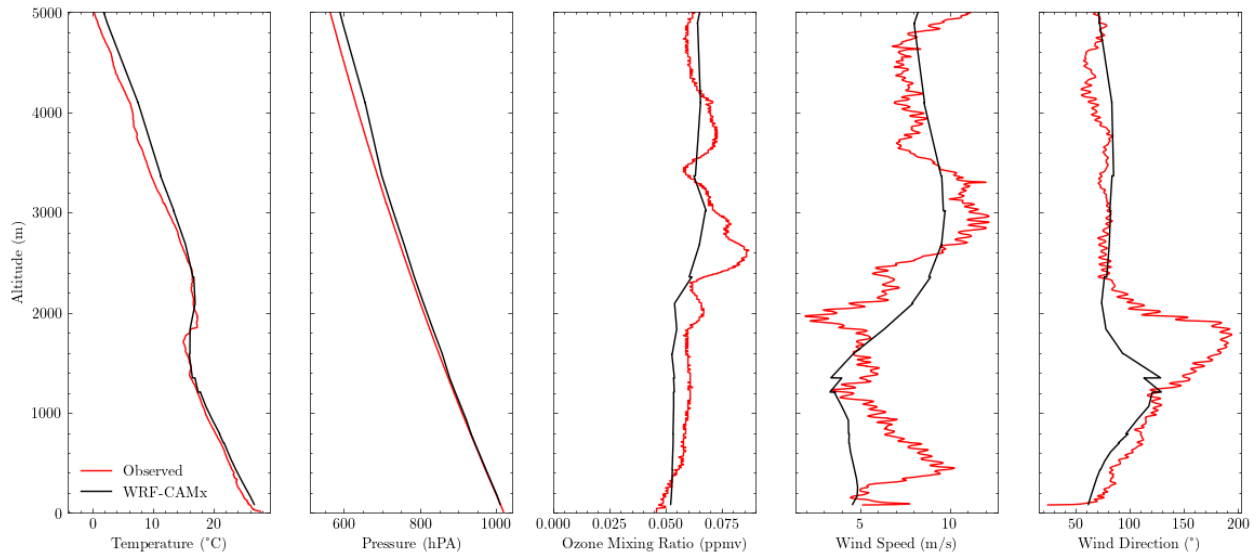


Figure S17: Comparison between WRF-CAMx simulated meteorology and ozone mixing ratios and ozonesondes observations at 9am on 9/11 at 29.67° N and 95.06° W (LaPorte)

150

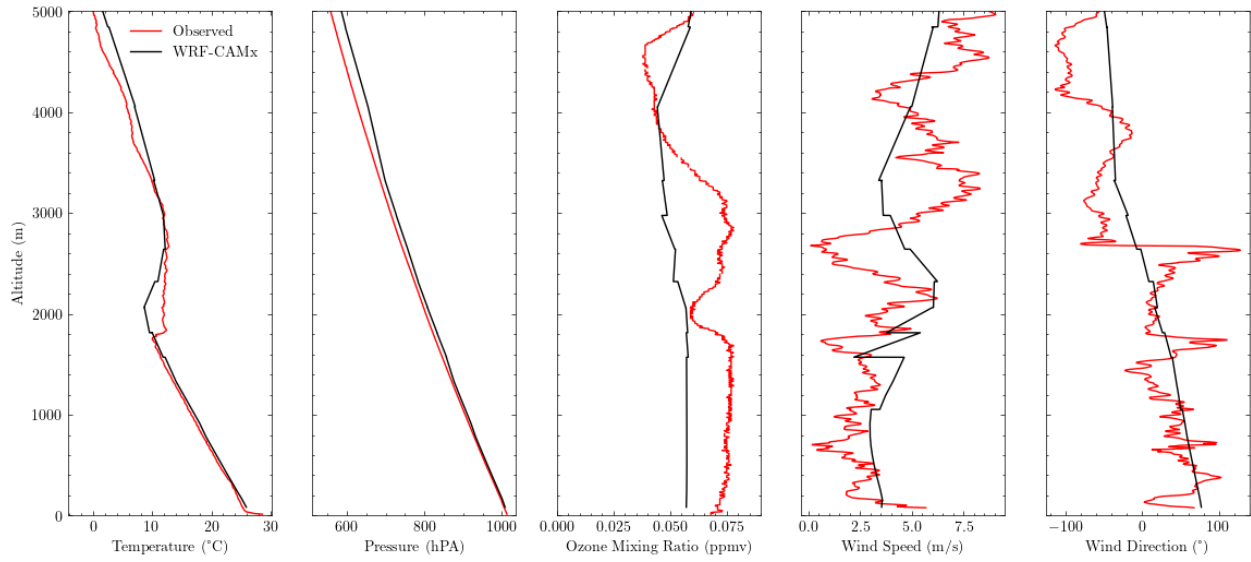


Figure S18: Comparison between WRF-CAMx simulated meteorology and ozone mixing ratios and ozonesondes observations at 1pm on 9/23 at 29.546° N and 95.53° W (Houston SW Airport)

155

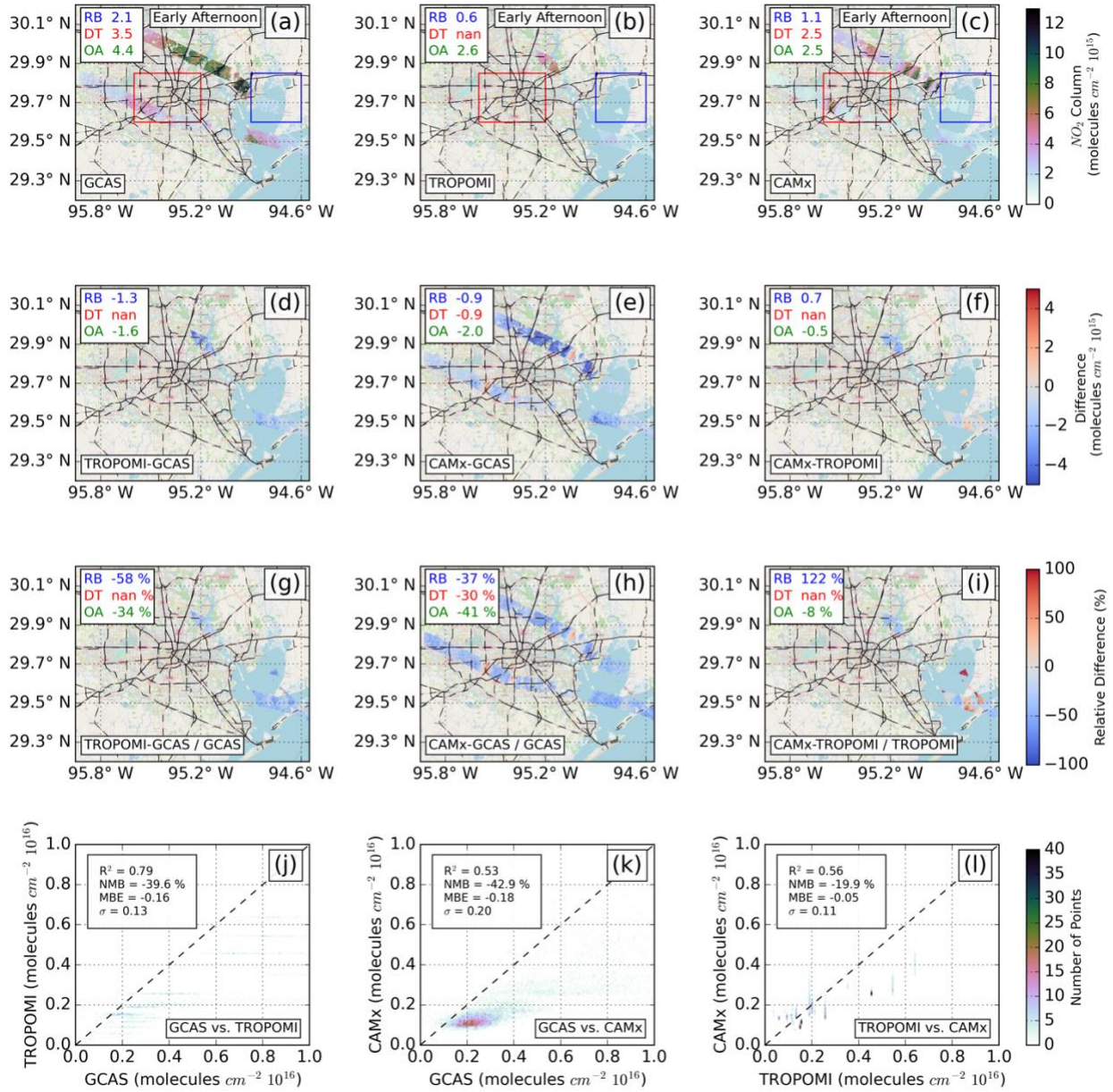
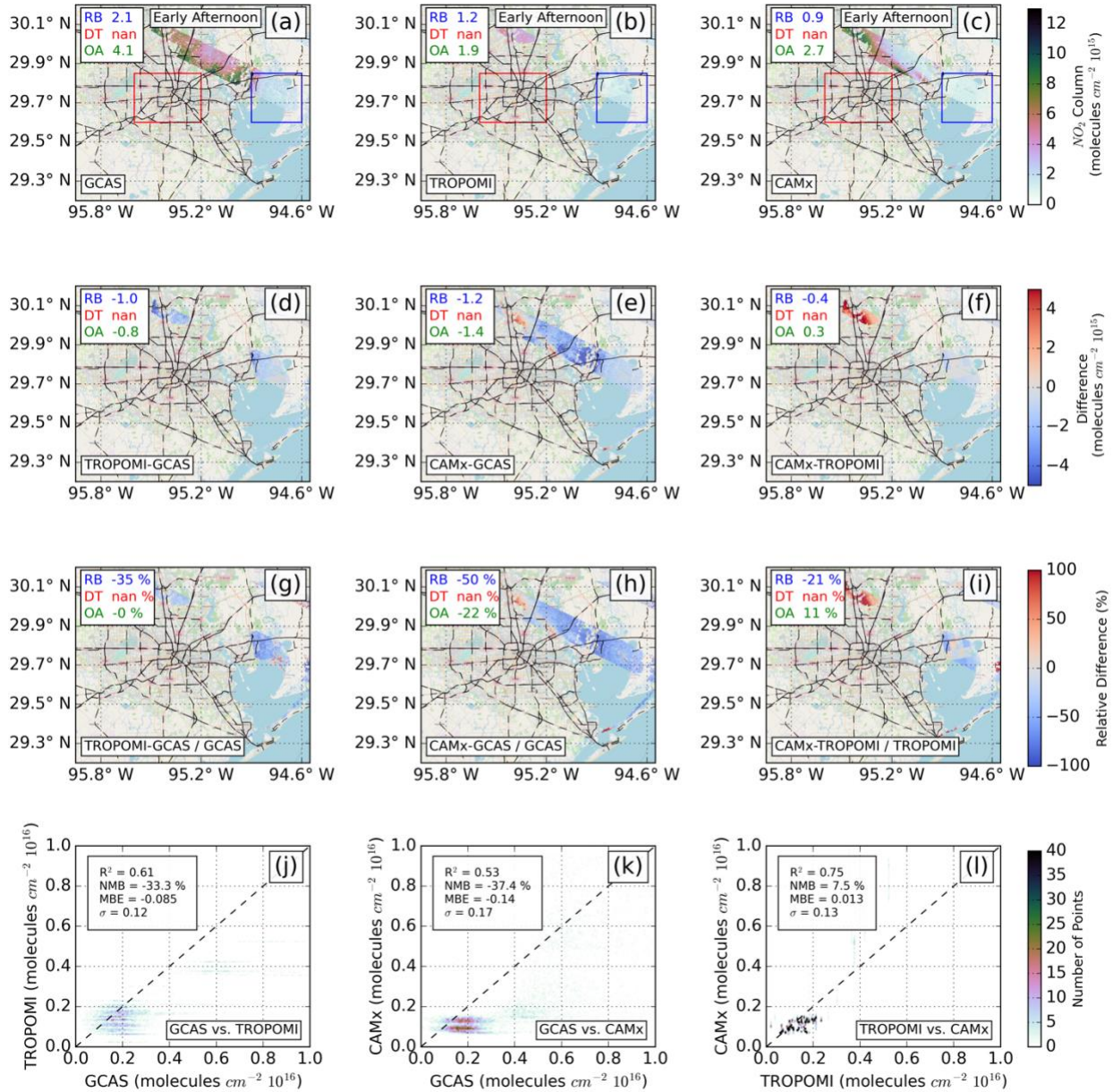


Figure S19: Spatial comparison of GCAS, TROPOMI, and CAMx on September 1, 2021. © OpenStreetMap contributors 2023. Distributed under the Open Data Commons Open Database License (ODbL) v1.0.



160 **Figure S20: Spatial comparison of GCAS, TROPOMI, and CAMx on September 3, 2021. © OpenStreetMap contributors 2023. Distributed under the Open Data Commons Open Database License (ODbL) v1.0.**

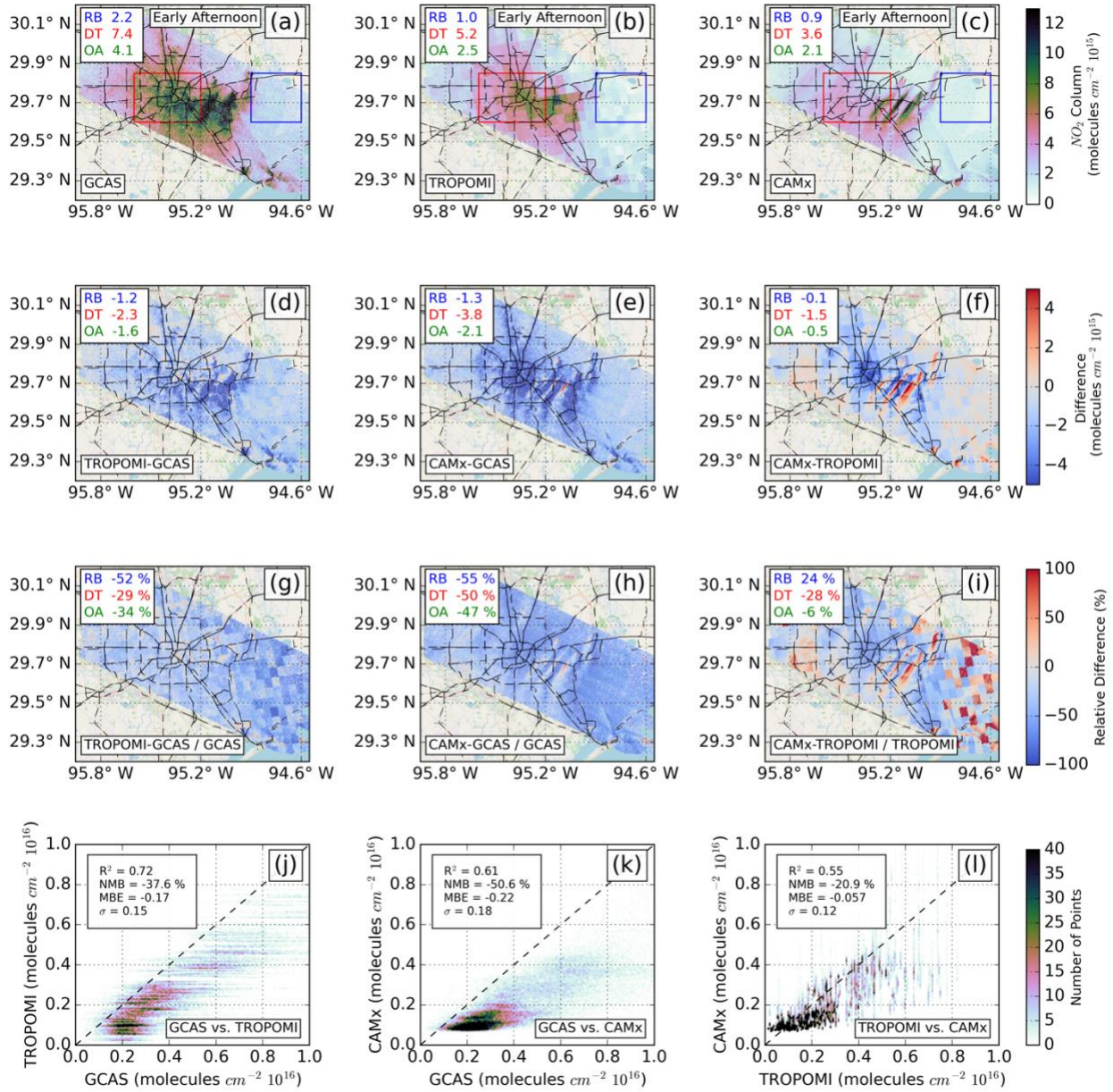
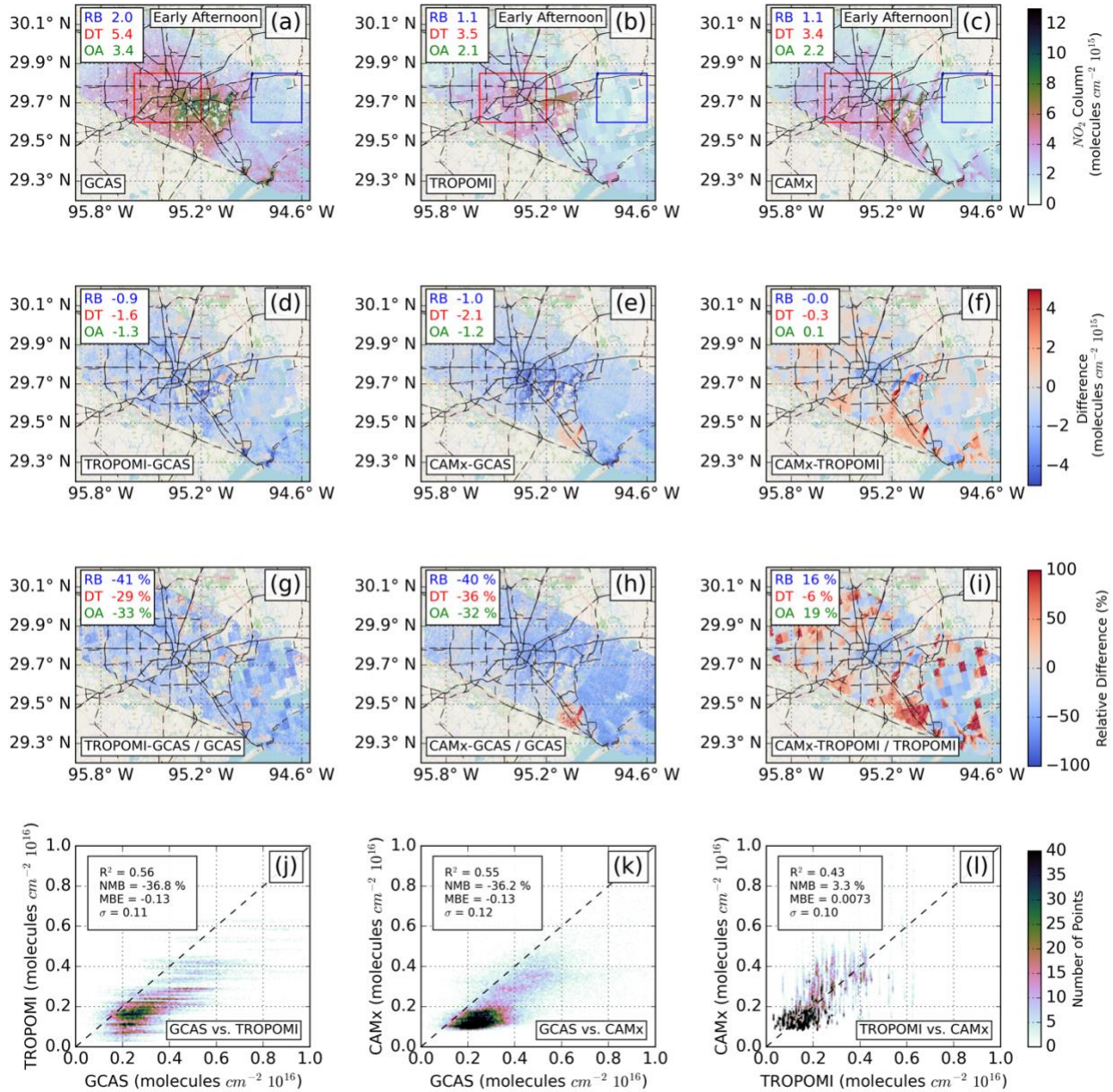
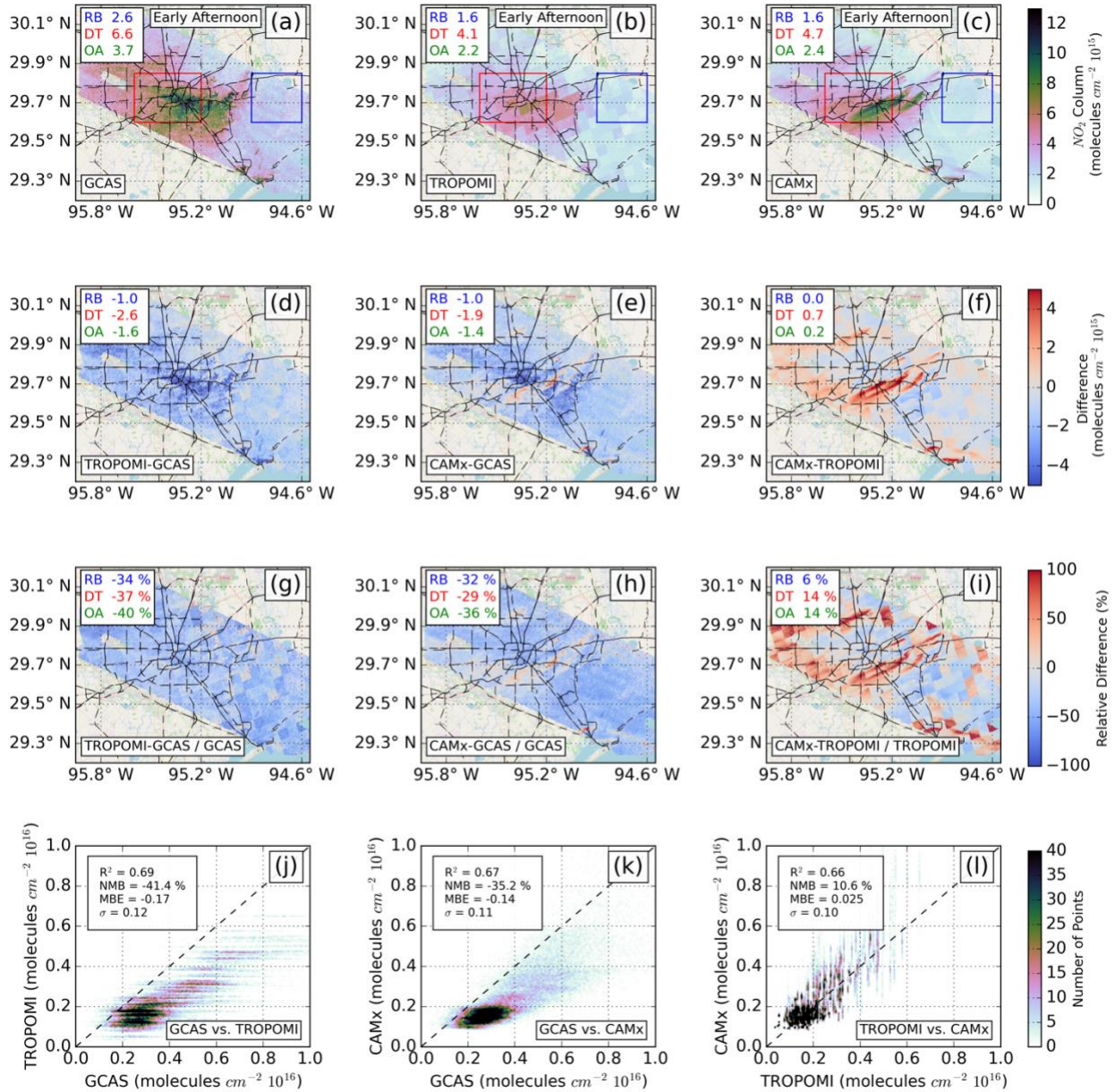


Figure S21: Spatial comparison of GCAS, TROPOMI, and CAMx on September 8, 2021. © OpenStreetMap contributors 2023. Distributed under the Open Data Commons Open Database License (ODbL) v1.0.



165

Figure S22: Spatial comparison of GCAS, TROPOMI, and CAMx on September 9, 2021. © OpenStreetMap contributors 2023. Distributed under the Open Data Commons Open Database License (ODbL) v1.0.



170 **Figure S23: Spatial comparison of GCAS, TROPOMI, and CAMx on September 10, 2021. © OpenStreetMap contributors 2023. Distributed under the Open Data Commons Open Database License (ODbL) v1.0.**

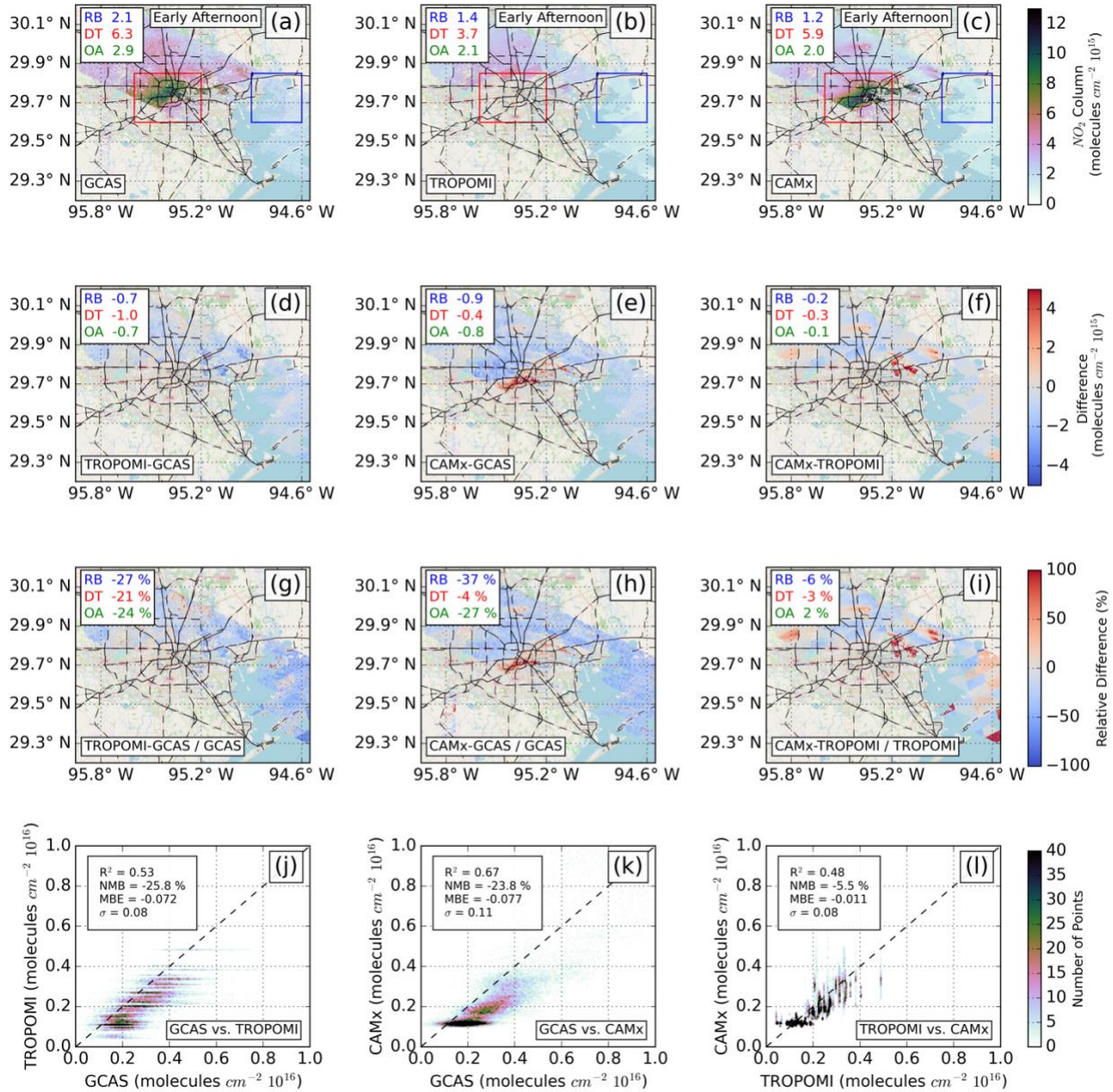
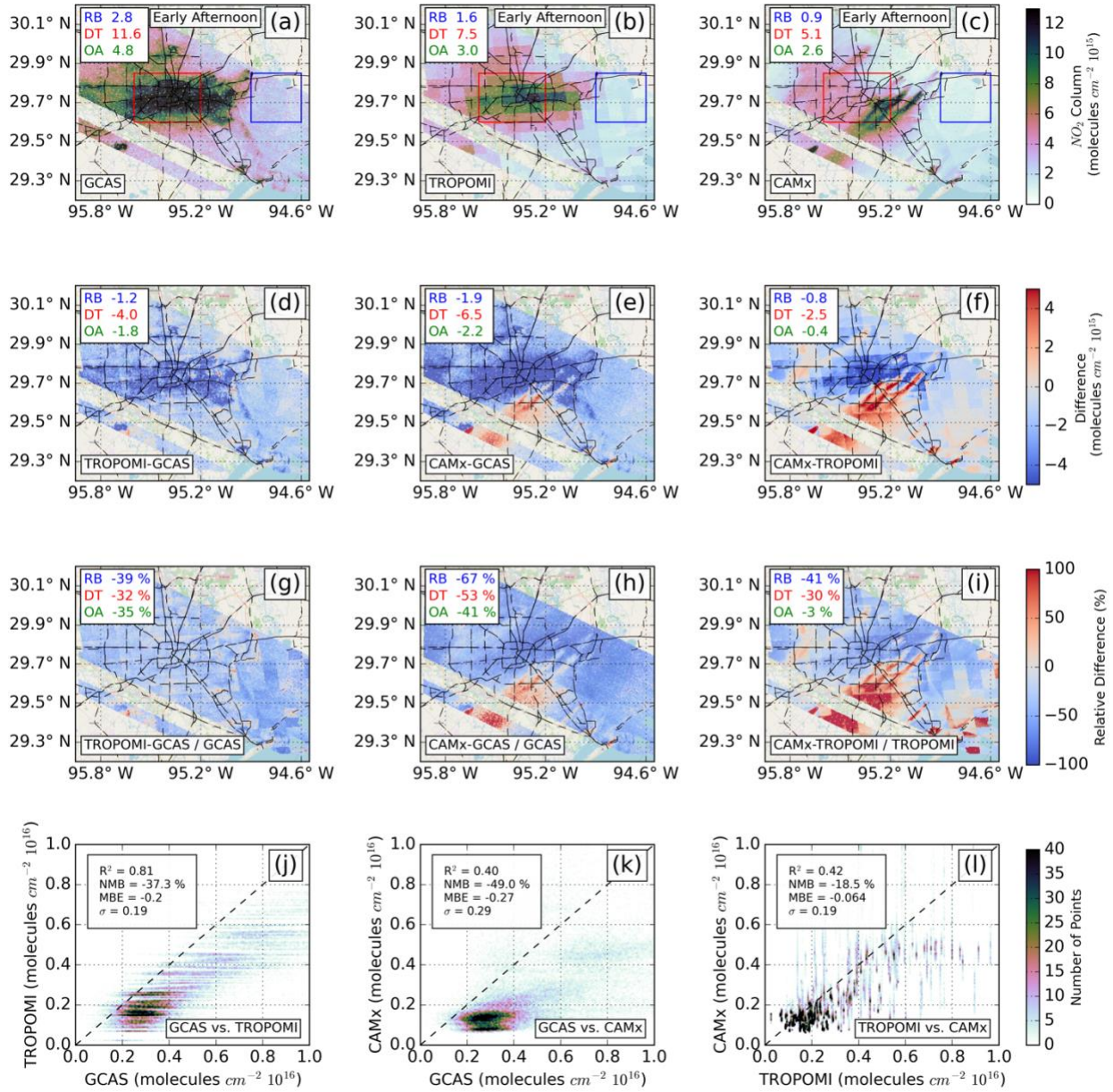


Figure S24: Spatial comparison of GCAS, TROPOMI, and CAMx on September 11, 2021. © OpenStreetMap contributors 2023. Distributed under the Open Data Commons Open Database License (ODbL) v1.0.



175 **Figure S25: Spatial comparison of GCAS, TROPOMI, and CAMx on September 23, 2021. © OpenStreetMap contributors 2023. Distributed under the Open Data Commons Open Database License (ODbL) v1.0.**

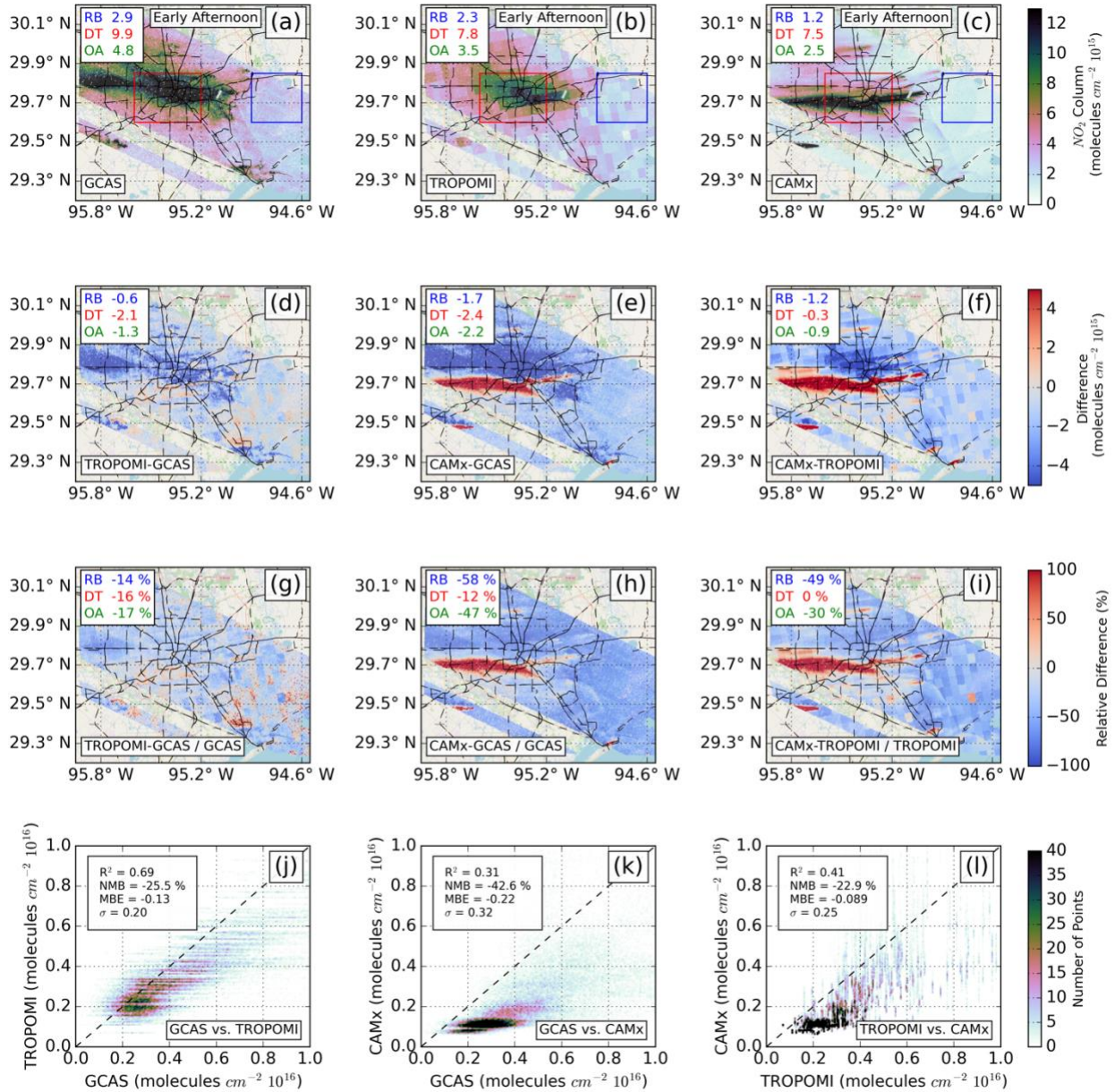
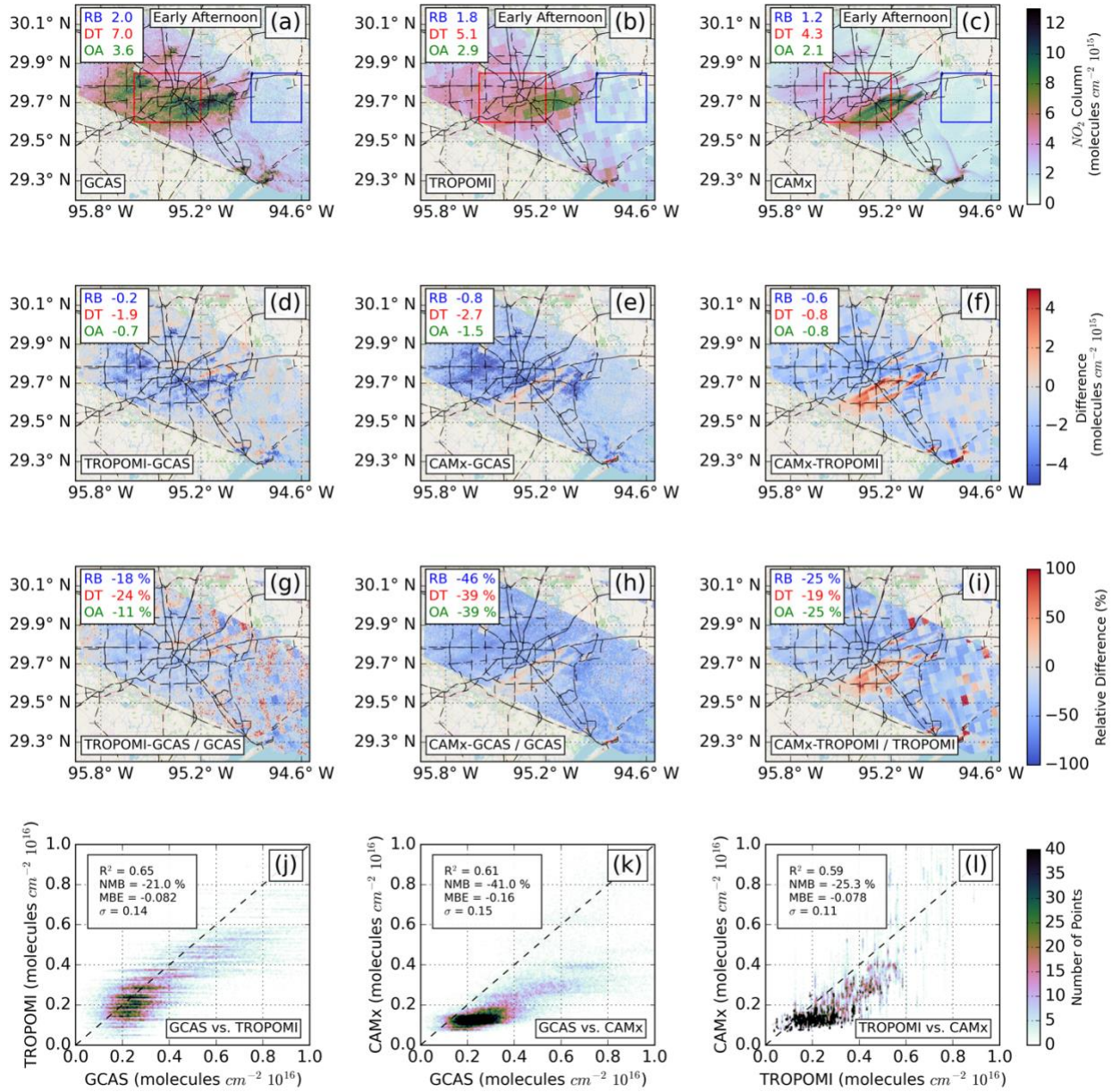
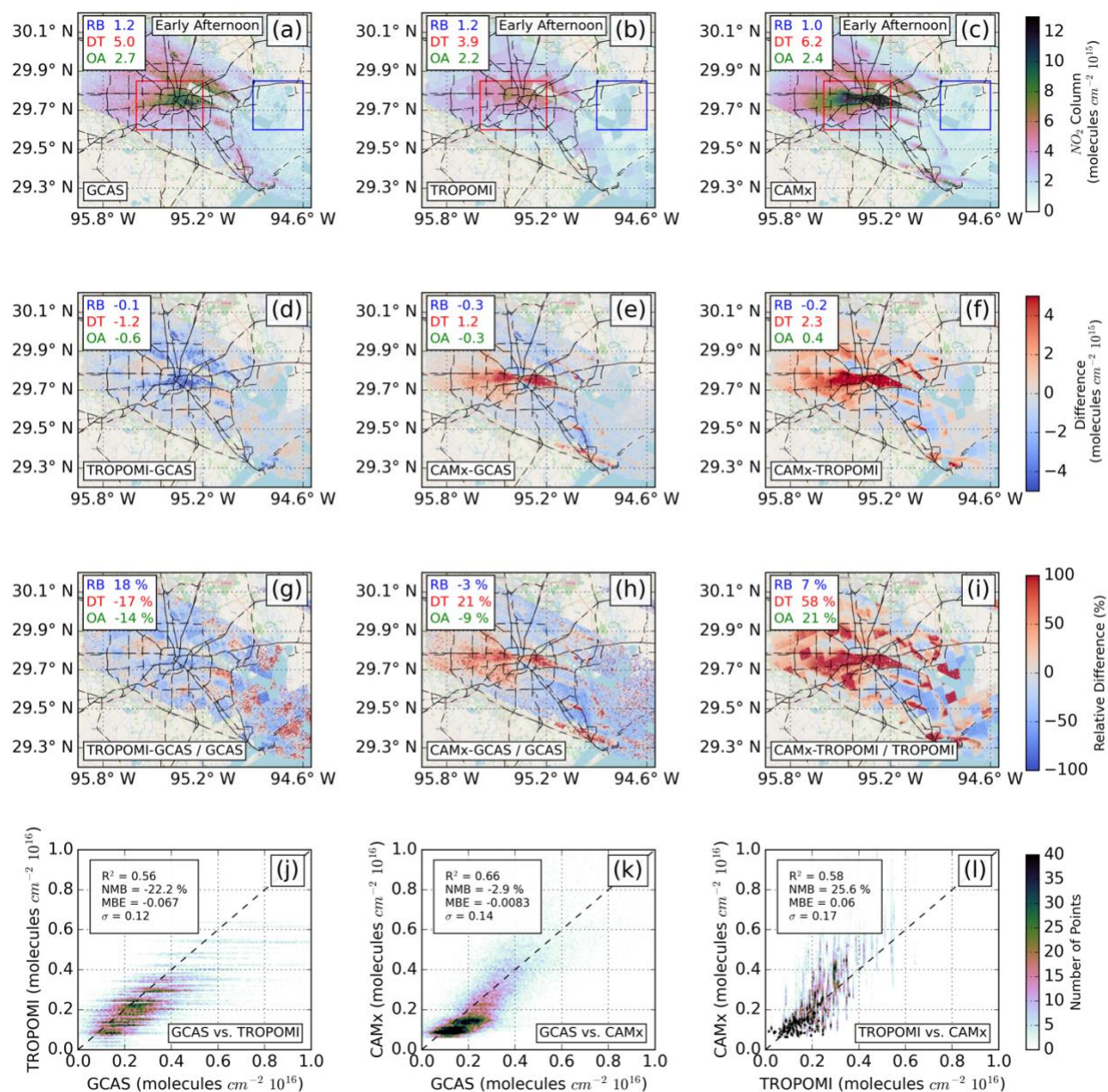


Figure S26: Spatial comparison of GCAS, TROPOMI, and CAMx on September 24, 2021. © OpenStreetMap contributors 2023. Distributed under the Open Data Commons Open Database License (ODbL) v1.0.



180

Figure S27: Spatial comparison of GCAS, TROPOMI, and CAMx on September 25, 2021. © OpenStreetMap contributors 2023. Distributed under the Open Data Commons Open Database License (ODbL) v1.0.



185

Figure S28: Spatial comparison of GCAS, TROPOMI, and CAMx on September 26, 2021. © OpenStreetMap contributors 2023. Distributed under the Open Data Commons Open Database License (ODbL) v1.0.

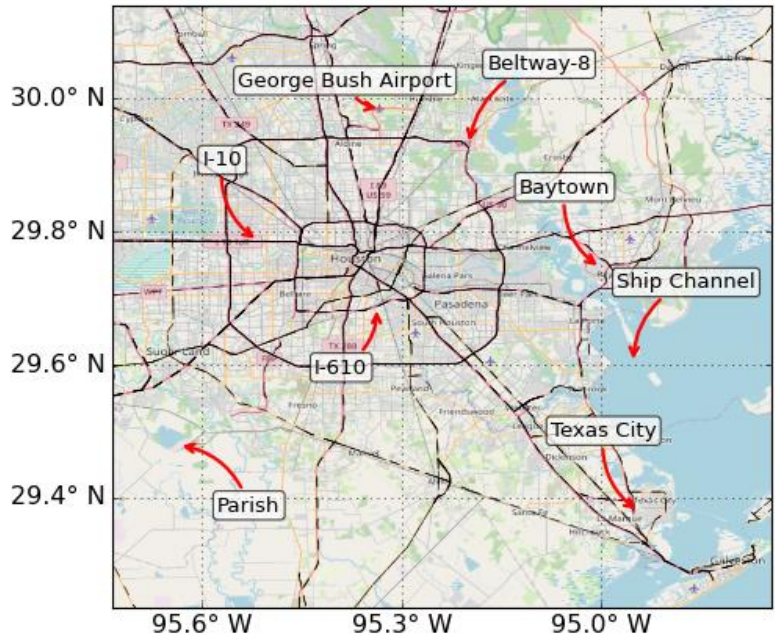


Figure S29: Map of notable features in and around Houston. © OpenStreetMap contributors 2023. Distributed under the Open Data Commons Open Database License (ODbL) v1.0.

190

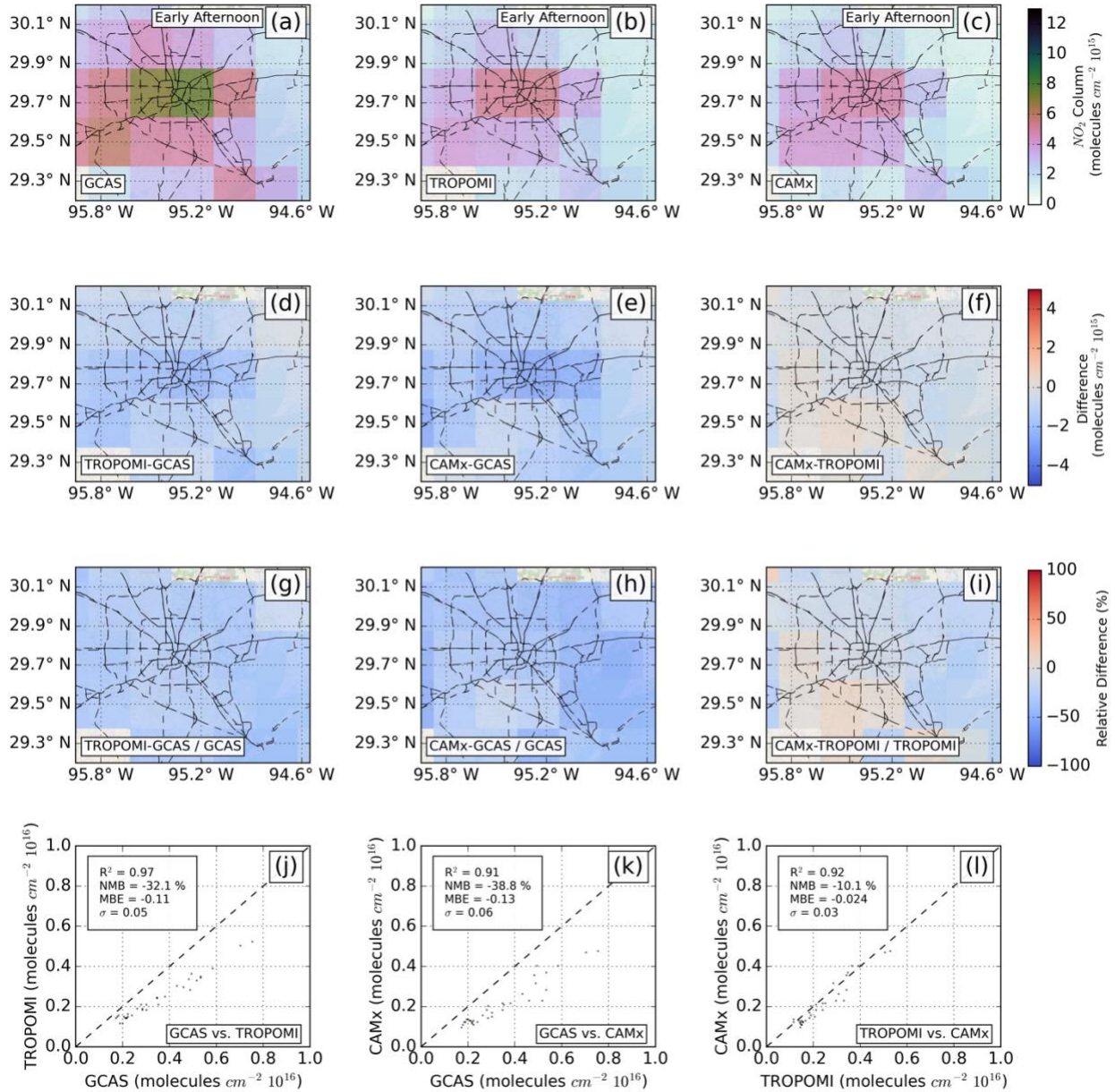
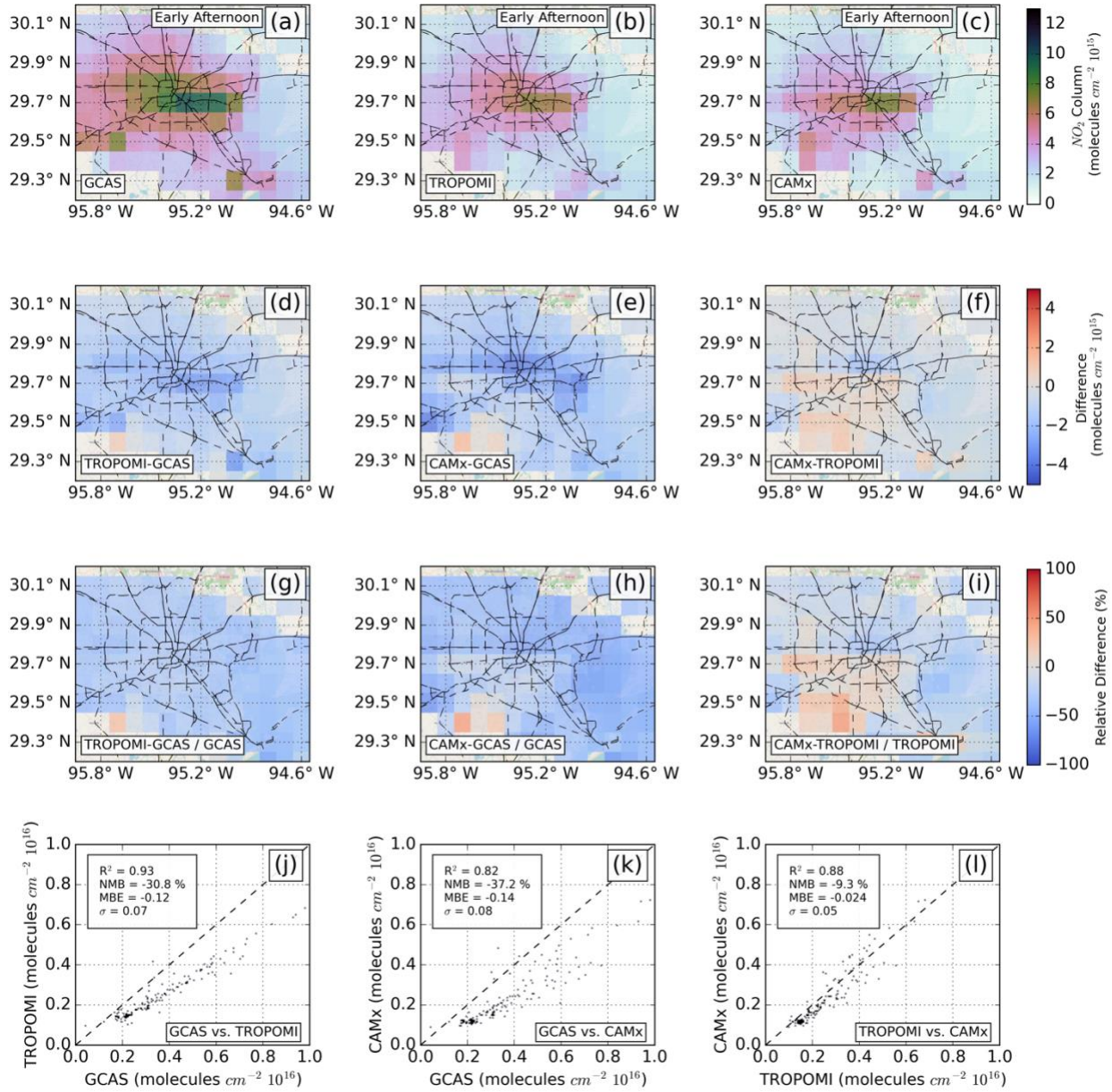


Figure S30: Spatial comparison of GCAS, TROPOMI, and CAMx at the $0.25^\circ \times 0.25^\circ$ resolution. © OpenStreetMap contributors 2023. Distributed under the Open Data Commons Open Database License (ODbL) v1.0.



195

Figure S31: Spatial comparison of GCAS, TROPOMI, and CAMx at the $0.1^\circ \times 0.1^\circ$ resolution. © OpenStreetMap contributors 2023. Distributed under the Open Data Commons Open Database License (ODbL) v1.0.

Section S2. Equations for statistics referenced in the main text

200

$$R^2 \text{ (Pearson-R squared): } R^2 = 1 - \frac{\sum(y_{obs} - y_{prd})^2}{\sum(y_{obs} - \bar{y}_{obs})^2}$$

$$\text{NMB (Normalized Mean Bias): } NMB = \frac{\sum(y_{prd} - y_{obs})}{\sum y_{obs}}$$

205

$$\text{MBE (Mean Bias Error): } MBE = \frac{1}{n} \sum (y_{prd} - y_{obs})$$

$$\text{MAE (Mean Absolute Error): } MAE = \frac{1}{n} \sum |y_{prd} - y_{obs}|$$

$$\sigma \text{ (Standard deviation of the residuals): } \sigma = \sqrt{\frac{\sum(r - \bar{r})^2}{n}}$$

210

y_{obs} : Data from the dataset suspected to be closest to truth (Pandora > GCAS > TROPOMI > CAMx)

y_{prd} : Data from the dataset suspected to be furthest from truth

\bar{y}_{obs} : Mean of y_{obs}

r : $y_{prd} - y_{obs}$

215

\bar{r} : Mean of r

n : Number of observations

220